J|A|C|S
ARTICLES
Published on Web 08/25/2006

Solvent-Induced Effects: Self-Association of Positively Charged π Systems

Eric Buisine,[†,‡] Katherine de Villiers,[§] Timothy J. Egan,[§] and Christophe Biot*[,||]

Contributions from the Laboratoire de Chimie Organique et Macromoléculaire, UMR CNRS 8009, Université des Sciences et Technologies, B.P. 90108, 59652, Villeneuve d'Ascq cedex, France, Ecole Nationale Supérieure de Chimie de Lille, B.P. 107, 59652, Villeneuve d'Ascq cedex, France, Department of Chemistry, University of Cape Town, Private Bag, Rondebosch 7701, South Africa, and Unité de Catalyse et Chimie du Solide - UMR CNRS 8181, Ecole Nationale Supérieure de Chimie de Lille, Bâtiment C7, USTL, B.P. 90108, 59652, Villeneuve d' Ascq cedex, France

Received March 23, 2006; E-mail: christophe.biot@ensc-lille.fr

Abstract: Antimalarial cationic drugs, such as chloroquine (CQ) and ferroquine (FQ), form stable dimer structures not only in the solid state but also in solution. The short distances (3.3−3.5 Å) observed between the positively charged quinolinium rings suggest that this self-association process is driven by π/π stacking interactions. Nevertheless, the strength of these dispersive forces is likely not sufficient to overcome the strong repulsive +/+ electrostatic effects. The question of the exact role of the environment, particularly the solvent, is clearly raised here. Characterization of these unconventional stabilizing nonbonding interactions which we have named $+\text{-}\pi/+\text{-}\pi$ is therefore of great importance. In the present work, we describe theoretical calculations and NMR experiments undertaken to probe the nature and the strength of $+\text{-}\pi/+\text{-}\pi$ interactions occurring upon self-association of FQ and CQ molecules in water.

Introduction

During the past two decades, the importance given to the study of nonbonding molecular interactions has rapidly increased due to the emergence and development of new concepts in molecular recognition and supramolecular chemistry.[1] A better understanding of these cooperative weak-intensity interactions is essential not only for biological investigations but also for rational drug design,[2] providing new insights into structure−activity relationships. As biological macromolecules and a large majority of drugs contain aromatic rings in their chemical structure, nonbonding interactions involving π electron systems are of particular importance. In this respect, the dispersive $\pi-\pi$ interactions commonly called $\pi-\pi$ stacking have been shown to play a crucial role both in the stability of proteins[3] or nucleic acids[4] and in the recognition of drugs by enzymes.[1b] Particular attention has also been devoted to the study of the interactions of cations with aromatic rings, including cation-π interactions.[5] Numerous experimental studies have emphasized the presence and the importance of these two major nonbonding forces, and a myriad of theoretical approaches have attempted to elucidate their true nature.[5] Beside these well characterized conventional interactions, the stability of unusual associations observed in aqueous environments between positively charged π systems has been reported.[6−8] While the $\pi-\pi$ dispersive forces present in such associations have an undeniable stabilizing effect, their strength is likely not sufficient to overcome the strong repulsive +/+ electrostatic effects. Hence, the question of the exact role of the environment (solvent, counterions, crystal packing) is clearly raised. Characterization of such unconventional nonbonding interactions which we have called $+\text{-}\pi/+\text{-}\pi$ is thus of great importance.

In this context, the propensity of diprotonated antimalarial drugs ferroquine[9] (FQ, SR97276) and chloroquine (CQ) (Figure 1) to form stable dimer structures in the presence of a polar solvent[10] or in the solid state has been observed.[11,12] As

[†] Laboratoire de Chimie Organique et Macromoléculaire.
[‡] Ecole Nationale Supérieure de Chimie de Lille.
[§] University of Cape Town.
[||] Unité de Catalyse et Chimie du Solide, Ecole Nationale Supérieure de Chimie de Lille.

(1) (a) Muller-Dethlefs, K.; Hobza, P. *Chem. Rev.* **2000**, *100*, 143−168. (b) Meyer, E. A.; Castellano, R. K.; Diederich, F. *Angew. Chem., Int. Ed.* **2003**, *42*, 1210−1250.
(2) Babine, R. E.; Bender, S. L. *Chem. Rev.* **1997**, *97*, 1359−1472.
(3) McGaughey, G. R.; Gagné, M.; Rappé, A. K. *J. Biol. Chem.* **1998**, *273*, 15458−15463.
(4) (a) Hobza, P.; Sponer, J. *Chem. Rev.* **1999**, *99*, 3247−3276. (b) Sponer, J.; Jurecka, P.; Marchan, I.; Luque, F.J.; Orozco, M.; Hobza, P. *Chemistry* **2006**, *12*, 2854−2865.
(5) (a) Ma, J. C.; Dougherty, D. A. *Chem. Rev.* **1997**, *97*, 1303−1324, and more recently, see: (b) Biot, C.; Wintjens, R.; Rooman, M. *J. Am. Chem. Soc.* **2004**, *126*, 6220−6221. (c) Sorme, P.; Arnoux, P.; Kahl-Knutsson, B.; Leffler, H.; Rini, J. M.; Nilsson, U. J. *J. Am. Chem. Soc.* **2005**, *127*, 1737−1743. (d) Hughes, R. M.; Waters, M. L. *J. Am. Chem. Soc.* **2005**, *127*, 6518−6519.
(6) No, K. T.; Nam, K.-Y.; Scheraga, H. A. *J. Am. Chem. Soc.* **1997**, *119*, 12917−12922.
(7) Spackova, N.; Berger, I.; Egli, M.; Sponer, J. *J. Am. Chem. Soc.* **1998**, *120*, 6147−6151.
(8) (a) Scherlis, D. A.; Marzari, N. *J. Phys. Chem. B* **2004**, *108*, 17791−17795. (b) Scherlis, D. A.; Marzari, N. *J. Am. Chem. Soc.* **2005**, *127*, 3207−3212.
(9) Biot, C. *Curr. Med. Chem.*: *Anti-Infect. Agents* **2004**, *3*, 135−147.
(10) Casabianca, L. B.; de Dios, A. C. *J. Phys. Chem. A* **2004**, *108*, 8505−8513.
(11) Biot, C.; Taramelli, D.; Forfar-Bares, I.; Maciejewski, L. A.; Boyce, M.; Nowogrocki, G.; Brocard, J. S.; Basilico, N.; Olliaro, P.; Egan, T. J. *Mol. Pharm.* **2005**, *2*, 185−193.
(12) Karle, J. M.; Karle, I. *Acta Crystallogr.* **1988**, *C44*, 1605-1608.

10.1021/ja061755u CCC: $33.50

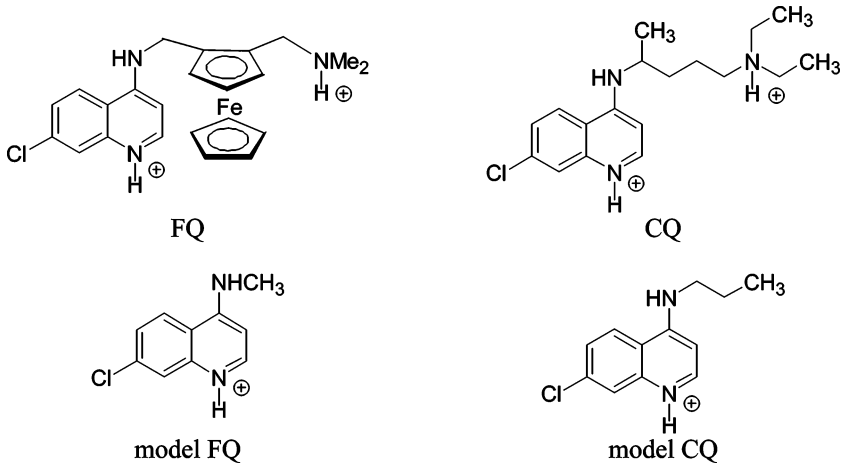

Figure 1. Structures of diprotonated ferroquine (FQ) and chloroquine (CQ) and their corresponding monoprotonated models.

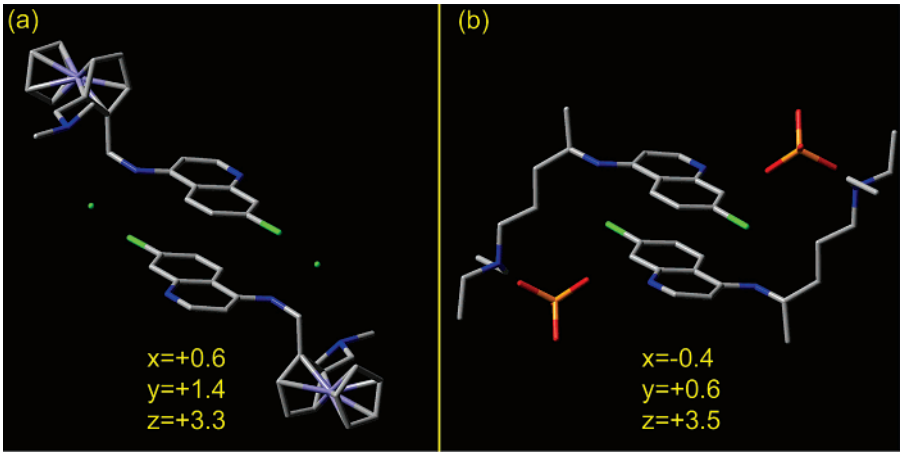

Figure 2. Stacking of quinolinium rings in crystal structures of diprotonated FQ (a) and CQ (b) molecules.[11,12] The counterions, namely chloride anions (green spheres) and dihydrogen phosphate groups, closest to the protonated basic amines are shown. Hydrogen atoms and water molecules have been omitted for clarity. X-ray data are available at the Cambridge Structural Database (Cambridge, UK).

evidenced by the crystallographic structures of FQ (Figure 2a) and CQ (Figure 2b), this self-association process involves primary face-to-face interactions of two positively charged quinolinium aromatic rings. Here, we present theoretical calculations and NMR experiments engaged to probe the nature and the strength of $+$-π/$+$-π interactions occurring upon the self-association of FQ and CQ molecules in water.

Computational Methods

Simplified Representation of FQ and CQ Molecules. According to both crystallographic[11,12] and NMR data[10] of FQ and CQ, neither the positively charged lateral amino side chains nor their associated counteranions (namely chloride ions and dihydrogen phosphate groups) seem to play a significant role in the internal cohesion of the dimer (Figure 2). Model monomer structures suitable for computational studies of quinolinium/quinolinium interactions were then considered for both FQ and CQ molecules (Figure 1). The counteranions were omitted and the side chains of the quinolinium core were truncated, leading to singly protonated (quinolinium) model structures. In the X-ray structure of FQ, the ferrocenyl side chain is almost perpendicular to the quinolinium ring and occupies specifically one side of the molecular π-plane.[11] The self-association process of FQ occurs through the unhindered π-face, so that the ferrocenyl side chain does not interfere with quinolinium ring stacking. Hence, the amino side chain of FQ has been simply replaced by a methyl group. In the case of CQ, both sides of the quinolinium ring are sterically hindered, one by the methyl group bound to carbon CH, the other one by the butyl amino side chain. As the dimerization process of CQ involves the more hindered face of the quinolinium ring, a propyl group was used in the model structure to mimic the aliphatic part of the side chain. Model monomer structures were optimized using the Hartree−Fock method (HF) and the 6-31g-(d) basis set. Truncated side chains of FQ and CQ were finally placed in their conformations as observed in the respective crystals.

Ab Initio Quantum Mechanics Energy Calculations. The energy landscapes of FQ and CQ dimers in water were first screened according to a classical grid approach (Figure 3). All energy calculations were carried out using the Gaussian 03 suite of programs.[13] For the building of the grids, the two corresponding model monomers were considered in an antiparallel-displaced mode of association and at an interplane separation distance of $z = 3.5$ Å. Indeed in organic molecular crystals, many aromatic molecules tend to be stacked with an interplane separation in the range 3.3−3.6 Å.[14] The upper quinolinium ring was shifted with respect to the lower by modifying incrementally its (x,y) coordinates as defined in Figure 3. The x coordinate was varied in the range -1.4 to $+1.4$ Å with a step size of 0.35 Å. The y coordinate was varied in the range -2.4 to $+2.4$ Å with a step size of 0.30 Å. The resulting conformational energy maps presented for the dimers of FQ and CQ were generated with the Origin software version 6.0 (Microcal Soft., Inc; Northampton, MA).

Grid point gas-phase energies were obtained by single-point calculations performed at the second order of the Møller-Plesset (MP2)

(13) Frisch et al. *Gaussian 03*, revision B. 05; Gaussian, Inc.: Wallingford, CT, 2004.
(14) Dahl, T. *Acta Chem. Scand.* **1994**, *48*, 95−116.

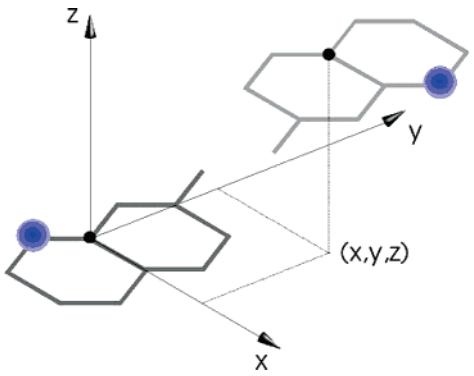

Figure 3. Coordinates (*x*,*y*,*z*) in Å defining the relative position of the two quinolinium rings used for the theoretical conformational investigations, assuming a similar antiparallel displaced mode of association as observed in the crystal structure.

perturbation theory[15] using the 6-31g(d) basis set. The MP2 energies were calculated as the sum of the Hartree−Fock (HF) energy E_{HF} and the electron correlation energy E_{Cor}:

$$E_{gas} = E_{MP2} = E_{HF} + E_{Cor}$$

The energies in water E_{water} were obtained by adding the corresponding solvation free energy ΔG_{water}:

$$E_{water} = E_{MP2} + \Delta G_{water}$$

The solvation free energies were calculated according to the IEF-PCM method described below.[16]

Finally, at the lowest energy points obtained from the FQ and CQ two-dimensional grids, the interplane separation distance *z* was optimized. The *z* coordinate was varied incrementally in the restricted range 3.0 to 3.7 Å with a step size of 0.1 Å. As the interplane separation distance may significantly affect the calculated energies, especially the dispersive contribution, the MP2 energies were here corrected for the basis set superposition error (BSSE). The BSSE corrections were performed using the standard counterpoise methods of Boys and Bernardi.[17]

Self-Association Energies. The FQ and CQ dimer geometries (Figure SI1 and Table SI1) used to estimate self-association energies and equilibrium constants were those issued from the grid-based approach and having the lowest MP2/6-31g(d)/IEF-PCM energies. Self-association energies in water ΔE_{water} were defined as the difference between energies of the $+\text{-}\pi/+\text{-}\pi$ dimers and those of the two $+\text{-}\pi$ separated monomers:

$$\Delta E_{water} = E_{water}(+\text{-}\pi/+\text{-}\pi) - 2E_{water}(+\text{-}\pi)$$

To obtain accurate self-association energies, MP2 energies were calculated with the extended basis sets 6-31+g(d), 6-31+g(d,p), 6-311+g(d,p), and 6-311++g(d,p) (Tables SI2 and SI3). All the dimer energies were corrected for the BSSE.[17] ZPE corrections were estimated in the gas phase at the HF/6-31g(d) level. Dimer geometries considered for frequency calculations were those arising from the grid approach and having the lowest MP2/IEF-PCM energies.

Solvent Effects. Aqueous solvation effects were modeled using the integral equation formalism (IEF) version of the polarizable continuum model (PCM).[16] The free energy of molecular systems were expressed as

$$G_{water} = G_{gas} + \Delta G_{water}$$

G_{gas} is the gas-phase free energy. Practically G_{gas} is often reduced to its pure electronic component (E_{gas}) calculated by quantum mechanical means. G_{gas} should indeed rigorously include other terms depending on solute atomic motions such as vibrational and rotational free energies.

ΔG_{water} represents the free solvation energy and reflects solute−water interactions. In continuum solvation models, the solvent is represented by a dielectric continuum and the solute molecule is embedded into a cavity. In this context, solvation energies are expressed as the sum of three terms:

$$\Delta G_{water} = \Delta G_{ele} + \Delta G_{dis-rep} + \Delta G_{cav}$$

$$\Delta G_{water} = \Delta G_{ele} + \Delta G_{non-ele}$$

The first term ΔG_{ele} represents the solute−solvent electrostatic contribution. $\Delta G_{dis-rep}$ is the dispersion-repulsion free energy, and ΔG_{cav} is the cavitation free energy. ΔG_{cav} corresponds to the reversible work needed to create the solute cavity in the solvent dielectric. The last two terms are often collectively referred to as the nonelectrostatic contribution ($\Delta G_{non-ele}$), as they do not affect the electronic distribution of the solute. In PCM calculations, the choice of the cavity is important because the computed energies and properties strongly depend on the cavity size. In this study, the aqueous solvation effects were evaluated with the three cavities BONDI, UAHF, and UA0 as implemented in the Gaussian 03 software. The UAHF and UA0 cavities use the united atom topological model where hydrogen atoms have no individual sphere but are included in the same sphere of the heavy atom they are bonded to. The UA0 cavity applies this model on atomic radii of the universal force field (UFF),[18] while the UAHF cavity applies it to atomic radii optimized for the HF/6-31g(d) level of theory.[19] For the BONDI cavity, explicit spheres using Bondi[20] atomic radii are assigned to each solute atom (heavy or hydrogen). For the electrostatic solvation terms, by default the PCM procedure scales the atomic radii by a factor equal to 1.2. This choice is justified by considering the fact that the first solvation layer does not have the same dielectric properties as the bulk of the solvent.[19] The free energies of solvation were calculated at the temperature 298.15 K with the dielectric constant $\epsilon = 78.39$.

The energy of self-association of FQ or CQ molecules in water (ΔE_{water}) was calculated by the addition of the energy of self-association in the gas phase estimated at the MP2 level (ΔE_{MP2}) to the difference ($\Delta\Delta G_{water}$):

$$\Delta E_{water} = \Delta E_{MP2} + \Delta\Delta G_{water}$$

The energy difference $\Delta\Delta G_{water}$ corresponds to the difference between the solvation energy of the $+\text{-}\pi/+\text{-}\pi$ dimers and those of the two $+\text{-}\pi$ separated monomers:

$$\Delta\Delta G_{water} = \Delta G_{water}(+\text{-}\pi/+\text{-}\pi) - 2\Delta G_{water}(+\text{-}\pi)$$

^{1}H and ^{13}C NMR Studies. Salts of diprotonated FQ dihydrochloride and CQ diphosphate were used for NMR experiments. Stock solutions of FQ·2HCl (0.020 M) and CQ·$2H_3PO_4$ (0.290 M) were prepared in D_2O. A series of dilutions of each stock solution permitted the preparation of solutions with lower concentrations. A 1-mL aliquot of each of these solutions was transferred to a standard 5 mm NMR tube, and its ^{1}H and ^{13}C NMR spectra were recorded on a Varian Unity 400 MHz spectrometer at 303 K. The change in chemical shift with increasing drug concentration was determined for quinolinium carbons for both compounds, while the change in chemical shift was monitored for hydrogen nuclei only in the case of FQ. The range of concentrations

(15) (a) Møller, C.; Plesset, M. S. *Phys. Rev.* **1934**, *46*, 618−622. (b) Head-Gordon, M.; Pople, J. A.; Frisch M. J. *Chem. Phys. Lett.* **1988**, *153*, 503−506.
(16) (a) Tomasi, J.; Mennucci, B.; Cancès, E. *THEOCHEM* **1999**, *464*, 211−226. (b) Tomasi, J.; Mennucci, B.; Cammi, R. *Chem. Rev.* **2005**, *105*, 2999−3094.
(17) Boys, S. F.; Bernardi, F. *Mol. Phys.* **1970**, *19*, 553−566.
(18) Rappé, A. K.; Casewit, C. J.; Colwell, K. S.; Goddard, W. A., III; Skiff, W. M. *J. Am. Chem. Soc.* **1992**, *114*, 10024−10035.
(19) Barone, V.; Cossi, M.; Tomasi, J. *J. Chem. Phys.* **1997**, *107*, 3210−3221.
(20) Bondi, A. *J. Phys. Chem.* **1964**, *68*, 441−451.

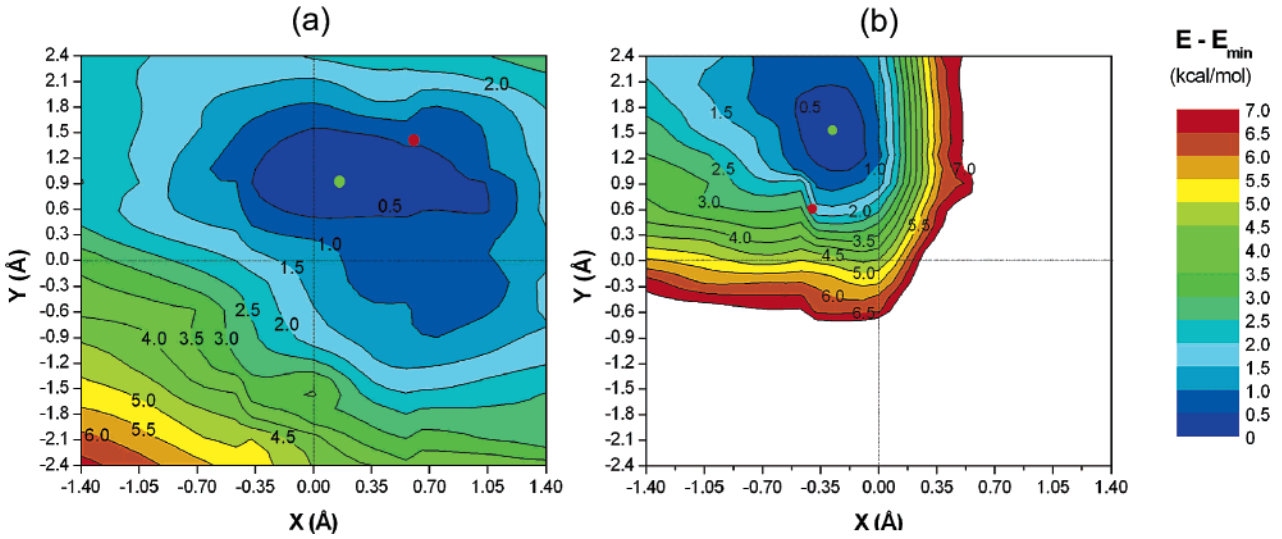

Figure 4. (x,y) relative conformational energy maps obtained for the FQ (a) and CQ (b) model dimers in water at the interplane distance $z = 3.5$ Å. The energy scale (in kcal/mol) is relative to the lowest calculated energy. The energy in water was calculated as the sum of the gas-phase energy (E_{MP2}) and the free energy of solvation in water (ΔG_{water}). The gas-phase energies were obtained at the second order of the Møller−Plesset (MP2) perturbation theory[15] using the 6-31g(d) basis set. The solvation free energies were calculated using the IEF polarizable continuum[16a] with the UAHF cavity. The X-ray FQ (x,y) coordinates and those of the lowest MP2 energy dimer are marked with a red and green dot, respectively.

were 0.007−0.290 M and 0.0002−0.020 M for CQ and FQ, respectively. The experimental data were fitted to the following equation:[10]

$$\delta_{obs} = \left[\left(\frac{-1 + \sqrt{1 + 8KC_t}}{4K}\right)/C_t\right](\delta_m - \delta_d) + \delta_d + YC_t$$

where δ_{obs} is the observed chemical shift, δ_m is the chemical shift of the monomer, δ_d is the chemical shift of the dimer, C_t is the total drug concentration, and K is the equilibrium constant of self-association. The linear term YC_t takes into account medium effects.[10] This linear term was only considered in extrapolations using ^{1}H NMR data.

Results and Discussion

In a first step, our theoretical strategy performed according to a classical grid approach allowed us to identify lowest energy conformations for FQ and CQ model dimers in water. The conformational energy maps obtained for the FQ and CQ model dimers at the interplane distance $z = 3.5$ Å using the UAHF cavity are shown in Figure 4. Energy maps generated for the BONDI and UA0 cavities are available in the Supporting Information (Figures SI2 and SI3). It is striking to see how the choice of the cavity does not affect the relative energy profile and that a unique minimum energy region always emerged. In the case of CQ, less flat minima were obtained due to the presence of the aliphatic side chain and the mode of stacking involving the most buried π-face of the quinolinium rings. In the lowest energy geometries, the upper quinolinium ring has an offset in the $+x$ and $+y$ directions for FQ and in the $-x$ and $+y$ directions for CQ. Interestingly, these offsets are similar to those observed in the crystal structures. In Figure 4, the X-ray (x,y) coordinates and those corresponding to the lowest energy dimers are marked with red and green dots, respectively. From the predicted (x,y) offsets, the interplane separation distance z was finally optimized. The most stable three-dimensional geometries obtained turned out to be very close to those observed in the X-ray structures. For FQ, the most stable predicted (x,y,z) geometry was (+0.35, +0.95, +3.3) versus (+0.6, +1.4, +3.3) in the crystallographic structure. In the case of CQ, the theoretical coordinates were (−0.2, +1.3, +3.4) versus (−0.4, +0.6, +3.5) in the solid state. From a theoretical point of view, these results validate the choice of our strategy and the proposed model structures, since, in our model monomers, side chains of quinolinium rings were truncated and counterions were omitted. More fundamentally, these results confirm that stacking of quinolinium rings is the main driving force in the self-association process of diprotonated FQ and CQ molecules.

In such +-π/+-π associations, the attractive $\pi-\pi$ dispersive forces commonly called $\pi-\pi$ stacking compete with the repulsive electrostatic forces exerted between positive charges. To have a reliable estimation of the balance between these two antagonistic forces, an accurate treatment of electronic correlations is needed. The +-π/+-π interaction energies of FQ and CQ were calculated at the *ab initio* MP2 level of theory using various basis sets (6-31g(d), 6-31+g(d), 6-31+g(d,p), 6-311+g(d,p), 6-311++g(d,p)) and corrected for the BSSE.[17] Note that this type of calculation appears to be the most appropriate, as density functional theory (DFT) methods fail completely for aromatic stacking representation,[4a,21] and highly computationally demanding nonperturbative coupled cluster (e.g., CCSD(T)) calculations are excluded due to the size of our model dimers. Moreover, the MP2 method has already proven successful in investigations of stacking of charged aromatic compounds.[22] Hence, Table 1 gives the MP2 interaction energy values obtained in the gas phase for the most extended 6-311++g(d,p) basis set. The dimer conformations used to estimate these self-association energies were those obtained from the initial grid-based approach (Figure SI1 and Table SI1). Results obtained with the basis sets 6-31g(d), 6-31+g(d), 6-31+g(d,p) and 6-311+g(d,p) are given in the Supporting Information (Tables SI2 and SI3).

Unsurprisingly, self-association energies (ΔE_{MP2}) of monoprotonated FQ and CQ models are strongly positive in the gas phase, viz. +41.4 and +39.2 kcal/mol, respectively. MP2 energies are expressed as the sum of the Hartree−Fock (HF)

(21) Hobza, P.; Sponer, J. *J. Am. Chem. Soc.* **2002**, *124*, 11802−11808.
(22) Scherlis, D. A.; Marzari, N. *J. Phys. Chem. B* **2004**, *108*, 17791−17795.

Table 1. Self-Association Energies (in kcal/mol) ΔE_{water} Using the 6-311++g(d,p) Basis Set

	ΔE_{HF}[a]	ΔE_{cor}[a]	ΔE_{ZPE}[b]	ΔE_{MP2}[a,c]	$\Delta\Delta G_{water}$[d]	ΔE_{water}
FQ	+63.4	−23.2	+1.3	+41.4	−45.0[e]	**−3.6**
					−53.2[f]	**−11.8**
CQ	+61.2	−23.3	+1.2	+39.2	−39.1[e]	**+0.1**
					−48.6[f]	**−9.5**

[a] Corrected for the BSSE and estimated by using the standard counterpoise method.[14] [b] Zero-point energy (ZPE) evaluated at the HF/6-31g(d) level of theory. [c] Corrected by the ZPE. [d] Values obtained from IEF-PCM[16a] calculations with the use of the two different cavities UAHF[e] and UA0[f].

energy ΔE_{HF} and the electron correlation energy ΔE_{cor}. The ΔE_{HF} energies are markedly positive due to strong +/+ electrostatic repulsions and, consequently, dominate over the negative electron correlation contributions ΔE_{cor}. The HF interaction energies for FQ and CQ models were found to be similar, viz. +63.4 and +61.2 kcal/mol, respectively, and were relatively stable with respect to the different basis sets. On the other hand, the accuracy of correlation energies depends on the size of the basis set, and the most negative values were obtained with the largest basis set. Addition of diffuse functions singularly improved the treatment of dispersive interactions (Tables SI1 and SI2). The correlation energies obtained with the 6-311++g(d,p) basis set were found identical for both FQ and CQ models, approximately −23 kcal/mol. Destabilizing electrostatic forces are thus preponderant, and despite attractive $\pi-\pi$ dispersive forces, the dimers of FQ and CQ are unstable in the gas phase. Therefore, to confirm the experimental observation that FQ and CQ molecules self-associate in an aqueous solution, solvation effects were considered, at least in a first attempt through an implicit approach.

Aqueous solvation effects were modeled using the integral equation formalism (IEF) version of the polarizable continuum model (PCM).[16] Continuum approaches are widely used as they offer the simplest methodology for incorporating solvent effects. PCM methods have been especially successful in the prediction of free energies of solvation of neutral solutes. Mean errors with respect to experimental data as low as 0.5 kcal/mol can be obtained.[19] On the other hand, the situation is generally far more difficult for ionic solutes with errors usually larger than 2 kcal/mol.[19] The main limitation of PCM methods arises in fact from the continuum approximation itself, e.g., the total absence of explicit solvent molecules. When specific short-range interactions are present between ionic solutes and the first shell of solvent molecules, the theoretical treatment is inevitably inadequate. In water, anions and cations have large free energies of hydration in the range 60−100 kcal/mol, while neutral molecules have values in the range 0−10 kcal/mol. Hence, any attempt to achieve an accuracy level of 1 kcal/mol in calculation of solvation energies (ΔG_{water}) of ions with continuum methods is clearly unrealistic. Finally, besides the validity of the continuum approximation itself, the accuracy of PCM solvation models depends on several factors. One of the most important is undoubtedly the cavity containing the solutes. The choice of cavity (shape, surface, and volume) is important, as computed energies and properties strongly depend on it. In the present work, three different cavity models were used: UA0, UAHF, and BONDI.

First of all, the IEF-PCM calculations using the BONDI cavity provide unsatisfactory results, since FQ and CQ model dimers were predicted unstable. Negative free energies of solvation $\Delta\Delta G_{water}$ were not able to reverse the overwhelming electrostatic−dispersive repulsive interaction. The sum of the gas-phase energy and free energy of solvation always results in a positive interaction energy (Tables SI2 and SI3). This corroborates previous observations on the incapacity of the BONDI cavity to correctly predict experimental free energies of hydration.[19] Hence, only values of free energies of solvation calculated with the UA0 and UAHF cavities have been considered and will be discussed in the following. In this respect, it is noteworthy that, for ionic solutes, the reliability of the UAHF model has been clearly proven.[19] The errors in the energies calculated with the UAHF cavity were indeed always found to be lower than the experimental uncertainty, e.g., 1−2 kcal/mol.

Solvent effects drastically affect the strength of FQ and CQ self-associations. Both model dimers are thus found to be strongly stabilized by immersion in the dielectric continuum. These strong stabilizing solvation effects can be qualitatively understood as a polarizable solvent favors the concentration of charges in smaller cavities.[8a] In our case, this cavity effect clearly enhances the stability of the doubly charged dimeric states compared to the isolated singly charged monomers. Table 1 gives the contribution of the solvation free energy (ΔG_{water}) to the energy of self-association (ΔE_{water}). FQ and CQ have large negative free energies of solvation. The most negative $\Delta\Delta G_{water}$ values are obtained with the UA0 cavity, −53.2 and −48.6 kcal/mol, respectively. With the UAHF cavity, computed values are approximately 8 to 9 kcal/mol higher than the previous ones ($\Delta\Delta G_{water}$ = −45.0 and −39.1 kcal/mol, respectively). These results show the extreme sensitivity of energy calculations to the shape and dimension of the cavity. Deviation from mean values arising from the use of the two cavities, viz −49.1 and −43.9 kcal/mol for FQ and CQ, respectively, is roughly 5 kcal/mol. However, with $\Delta\Delta G_{water} = \Delta G_{water}(\text{dimer}) - 2\Delta G_{water}(\text{monomer})$, this low accuracy is not surprising. Errors in $\Delta\Delta G_{water}$ energies could be indeed at least 3 times those in solvation energies (ΔG_{water}) computed for individual molecular species.

Finally, in the case of FQ and independently of the cavity model, the solvation energy reverses the balance from overall electrostatic-dispersive repulsion (ΔE_{MP2}) to attraction and *a priori* thermodynamic stability. Resulting ZPE-corrected self-association energies (ΔE_{water}) were thus −3.6 and −11.8 kcal/mol by use of the two UAHF and UA0 cavities, respectively. For CQ, the solvation free energy obtained with the UAHF cavity only just compensates the positive gas-phase contribution resulting in a self-association energy close to zero (ΔE_{water} = +0.1 kcal/mol). On the other hand, with the UA0 cavity, the self-association energy computed for CQ becomes large and negative (−9.5 kcal/mol). Despite this important difference in computed solvation energies, it is notable that both cavity models predict a similar difference between the interaction energies of FQ and CQ dimers (2.3 and 3.7 kcal/mol, respectively). Hence one can consider that the self-association of FQ in water is stronger than CQ.

In the PCM context, solvation energies are partitioned into an electrostatic and a nonelectrostatic term. The variation of the solvation free energy ($\Delta\Delta G_{water}$) from the two monomers to the stacked dimers is thus expressed as the sum of two independent components, ΔG_{ele} and $\Delta\Delta G_{non-ele}$. The $\Delta\Delta G_{ele}$

Table 2. Solvation Free Energy Decomposition Data for the Self-Association of Model FQ in Water[a]

z (Å)	$\Delta\Delta G_{water}$[b,c]	$\Delta\Delta G_{ele}$[b-d]	$\Delta\Delta G_{non-ele}$[b,c]	$\Delta\Delta G_{disp-rep}$[b,c]	$\Delta\Delta G_{cav}$[b,c]
3.3	−45.0	−50.7	+5.7	+10.0	−4.3
4.5	−35.4	−44.6	+9.2	+9.2	0.0

[a] The FQ model dimer is considered in its optimal quinolinium offset ($x = +0.35$, $y = +0.95$) at two interplane separation distances z, 3.3 and 4.5 Å, respectively. [b] $\Delta\Delta G_x = \Delta G_x(+\text{-}\pi/+\text{-}\pi) - 2\Delta G_x(+\text{-}\pi)$, where x stands for water, ele, non-ele, disp-rep, or cav. [c] Using IEF-PCM[16] calculations at 298.15 K with the UAHF cavity model. [d] Calculated at the HF/6-311++g(d,p) level of theory.

term represents the solute−solvent electrostatic contribution. The second gathers the two nonelectrostatic contributions, the dispersion-repulsion free energy ($\Delta\Delta G_{dis-rep}$), and the cavitation free energy ($\Delta\Delta G_{cav}$). The cavitation energy represents the amount of work required to form the cavity in the solvent. As previously noted[23] and confirmed further in the present study, the solute−solvent electrostatic interaction is the most important contribution to the free energy of solvation, especially in polar media and when ionic species are involved. The nonelectrostatic contribution is often regarded as playing only a minor role. The decomposition of solvation free energy calculated for FQ dimerization with the UAHF cavity is presented in Table 2. Similar results have been obtained with the UA0 cavity (data not shown). The energy decomposition highlights two essential trends. First, the strongly stabilizing effect of the electrostatic term is confirmed. The values of $\Delta\Delta G_{ele}$ obtained were large and negative, −50.7 and −44.6 kcal/mol, at the two considered interplane distances $z = 3.3$ and 4.5 Å, respectively.

As the concentration of charges is favored in the smaller cavities, a more negative value was logically obtained at the shortest distance. Second, compared to the electrostatic term, the nonelectrostatic component ($\Delta\Delta G_{non-ele}$) has only a moderate effect. Its $\Delta\Delta G_{disp-rep}$ component is positive and remains relatively stable with respect to the separation distance (roughly between 9 and 10 kcal/mol), being thus always unfavorable for the dimer stability. At the separation distance $z = 4.5$ Å, the values of $\Delta G_{disp-rep}$ and $\Delta\Delta G_{cav}$ obtained are +9.2 and 0.0 kcal/mol, respectively. In fact when the two monomers are infinitely separated, the dispersion-repulsion term represents the entirety of the nonelectrostatic term $\Delta\Delta G_{non-ele}$. On the other hand, upon stacking, the surface of the dimeric state with respect to the isolated monomers decreases and the energy of cavity formation ($\Delta\Delta G_{cav}$) becomes negative. At the minimal distance $z = 3.3$ Å, the monomers have close contact and the $\Delta\Delta G_{cav}$ corresponds in absolute value to ∼40% of the $\Delta\Delta G_{disp-rep}$. This result points out the crucial contribution of the cavitation free energy to the stability of the FQ model dimer. Despite its moderate value (∼ −4.3 kcal/mol), the cavitation term $\Delta\Delta G_{cav}$ is able to reverse the balance from overall electrostatic-dispersive repulsion to attraction and thermodynamic stability. For dimerization processes of small molecules in solution, the importance of the free energy of cavity formation had been already recognized.[23]

From the thermodynamic point of view, an accurate estimation of the self-association strength of FQ and CQ in water would require the knowledge of the related changes in Gibbs energies. A key step in the calculation of standard (1 M at 298.15 K) changes in Gibbs energy concerns without any doubt the solvent contribution, with the accuracy limitations described above, but also the unfavorable loss of conformational entropy accompanying the dimer formation. In this respect, it is noteworthy that the decrease of entropy arises not only from the loss of translational and rotational degrees of freedom inherent to the dimerization process but also from the restriction of the torsional flexibility of quinolinium side chains. For the present theoretical study, quinolinium side chains of FQ and CQ molecules were truncated and associated counteranions were omitted. Our aim was indeed simply to probe the nature and the strength of the $+\text{-}\pi/+\text{-}\pi$ interactions occurring upon quinolinium ring stacking. Hence, we considered that an estimation of individual self-association equilibrium constants from ΔE_{water} energy values would be unfounded. On the other hand, the difference of calculated energy in water ($\Delta\Delta E_{water}$) should provide a more reliable estimate of the relative stability of FQ and CQ dimers. With $\Delta\Delta E_{water} = \Delta E_{water}(FQ) - \Delta E_{water}(CQ)$, the equilibrium constant ratio can be expressed as $K_{FQ}/K_{CQ} = \exp(-\Delta\Delta E_{water}/RT)$. At the temperature 298.15 K, the average K_{FQ}/K_{CQ} is thus almost 300, being deduced from the individual values 49 and 517 obtained from solvation energies calculations using the two different cavities UA0 and UAHF, respectively.

To probe the relevance of our approximations and the limitations of these theoretical results, we investigated the strength of the FQ and CQ dimers formed in solution by means of NMR spectroscopy. The changes in the chemical shifts for quinolinium carbons and protons were monitored with increasing drug concentration (Figures SI4 and SI5). The log K value for CQ dimerization was determined for dilute solutions (0.007−0.290 M) and was found to be in the range 0.06 to 0.8. This corresponds to an average K value of 3 M^{-1} close to that of 5 M^{-1} which has previously been reported from proton data.[24] In the case of FQ, the determination of the equilibrium constant was more difficult to measure owing to limited solubility in water, probably arising from hydrophobic aggregation phenomena arising from the ferrocenyl moiety. Nevertheless, a reasonable estimate of the log K value was determined for dilute solutions (0.0002−0.020 M) and was found to lie in the range 2.5 to 3.3 giving an average K value of 800 M^{-1}. Thus, despite uncertainty in the precise dimerization constants, experimental data unequivocally confirm that the FQ dimerization constant is more than 2 orders of magnitude larger than that of CQ. This provides strong experimental support for the theoretical predictions described above. Indeed, the experimental ratio K_{FQ}/K_{CQ} of approximately 270 is in excellent agreement with its theoretically predicted average value of 300.

Conclusion

The self-association phenomenon observed for the cationic drugs FQ and CQ in the solid state and in an aqueous solution is singularly driven by $+\text{-}\pi/+\text{-}\pi$ nonbonding interactions. Our theoretical calculations provide an energetic insight of this unusual type of intermolecular force and highlights the crucial role of the solvent. The model dimer structures formed by stacking of quinolinium rings are clearly predicted to be unstable in the gas phase due to strong electrostatic-dispersive repulsion. On the other hand, solvent effects simulated with a polarizable continuum model are markedly stabilizing. The self-association

(23) Josefredo, R.; Pliego, J. R., Jr. *J. Braz. Chem. Soc.* **2005**, *16*, 227−231.

(24) Marchettini, N.; Valensin, G.; Gaggelli, E. *Biophys. Chem.* **1990**, *36*, 65−70.

of FQ in water was thus predicted to be thermodynamically favorable and stronger than CQ. The relative strength of FQ and CQ dimer molecules estimated from our theoretical considerations is moreover in agreement with that deduced from our NMR investigations. This property of positively charged π-rich systems to stack despite strong electrostatic repulsion in polar medium may explain why, in proteins, pairings of basic amino acid side chains such as arginines and histidines are so frequently observed. We are currently investigating how such $+$-π/$+$-π interactions can contribute to protein stability, protein/protein assemblies, and hence biological activities.

Acknowledgment. The NMR study is based upon work supported by the National Research Foundation of South Africa (2069079). KAdV further acknowledges the Department of Chemistry, University of Cape Town Equity Development Program for financial support.

Supporting Information Available: Lowest MP2/IEF-PCM energy conformations of FQ and CQ model dimers with their respective Cartesian coordinates. Basis-set dependence on self-association energies for FQ and CQ. Grid-based energy maps obtained for the FQ and CQ using the BONDI and UA0 cavities. Chemical shifts of carbons 8 and 9 of CQ and of carbon 2 and proton 2 of FQ at various concentrations. Complete ref 13. This material is available free of charge via the Internet at http://pubs.acs.org.

JA061755U